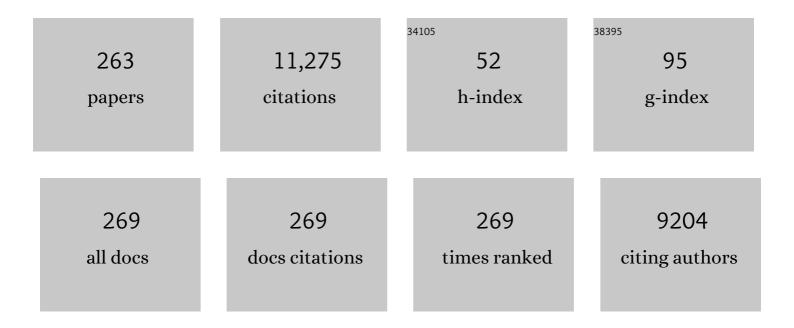
List of Publications by Year in descending order

Source: https://exaly.com/author-pdf/6503620/publications.pdf Version: 2024-02-01



REDNADD DAM

#	Article	IF	CITATIONS
1	Efficient solar water splitting by enhanced charge separation in a bismuth vanadate-silicon tandem photoelectrode. Nature Communications, 2013, 4, 2195.	12.8	1,137
2	The Origin of Slow Carrier Transport in BiVO ₄ Thin Film Photoanodes: A Time-Resolved Microwave Conductivity Study. Journal of Physical Chemistry Letters, 2013, 4, 2752-2757.	4.6	478
3	Origin of high critical currents in YBa2Cu3O7â^î´ superconducting thin films. Nature, 1999, 399, 439-442.	27.8	432
4	Evidence for mean free path fluctuation induced pinning inYBa2Cu3O7andYBa2Cu4O8films. Physical Review Letters, 1994, 72, 1910-1913.	7.8	301
5	Review of magnesium hydride-based materials: development and optimisation. Applied Physics A: Materials Science and Processing, 2016, 122, 1.	2.3	274
6	Pathways to electrochemical solar-hydrogen technologies. Energy and Environmental Science, 2018, 11, 2768-2783.	30.8	238
7	Metal–polymer hybrid nanomaterials for plasmonic ultrafast hydrogen detection. Nature Materials, 2019, 18, 489-495.	27.5	227
8	A Bismuth Vanadate–Cuprous Oxide Tandem Cell for Overall Solar Water Splitting. Journal of Physical Chemistry C, 2014, 118, 16959-16966.	3.1	226
9	Hydrogenography: An Optical Combinatorial Method To Find New Lightâ€Weight Hydrogen‧torage Materials. Advanced Materials, 2007, 19, 2813-2817.	21.0	186
10	Destabilization of the Mg-H System through Elastic Constraints. Physical Review Letters, 2009, 102, 226102.	7.8	157
11	Visualization of hydrogen migration in solids using switchable mirrors. Nature, 1998, 394, 656-658.	27.8	152
12	Efficient Water‧plitting Device Based on a Bismuth Vanadate Photoanode and Thinâ€Film Silicon Solar Cells. ChemSusChem, 2014, 7, 2832-2838.	6.8	149
13	Unraveling the Carrier Dynamics of BiVO ₄ : A Femtosecond to Microsecond Transient Absorption Study. Journal of Physical Chemistry C, 2014, 118, 27793-27800.	3.1	142
14	A reliable, sensitive and fast optical fiber hydrogen sensor based on surface plasmon resonance. Optics Express, 2013, 21, 382.	3.4	124
15	Vortex pinning by natural linear defects in thin films ofYBa2Cu3O7â~'δ. Physical Review B, 2001, 64, .	3.2	119
16	Structural, optical, and electrical properties ofMgyTi1â~'yHxthin films. Physical Review B, 2007, 75, .	3.2	116
17	Synthesis of yttriumtrihydride films for ex-situ measurements. Journal of Alloys and Compounds, 1996, 239, 158-171.	5.5	113
18	Hydriding kinetics of Pd capped YHx switchable mirrors. Journal of Applied Physics, 1999, 86, 6107-6119.	2.5	108

#	Article	IF	CITATIONS
19	Fiber optic hydrogen detectors containing Mg-based metal hydrides. Sensors and Actuators B: Chemical, 2007, 123, 538-545.	7.8	104
20	Critical current, magnetization relaxation and activation energies for YBa2Cu3O7 and YBa2Cu4O8 films. Physica C: Superconductivity and Its Applications, 1995, 241, 353-374.	1.2	102
21	Nanostructured materials for solid-state hydrogen storage: A review of the achievement of COST Action MP1103. International Journal of Hydrogen Energy, 2016, 41, 14404-14428.	7.1	94
22	Fiber optic Surface Plasmon Resonance sensor based on wavelength modulation for hydrogen sensing. Optics Express, 2011, 19, A1175.	3.4	93
23	A new thin film photochromic material: Oxygen-containing yttrium hydride. Solar Energy Materials and Solar Cells, 2011, 95, 3596-3599.	6.2	90
24	Natural strong pinning sites in laser-ablatedYBa2Cu3O7â^î thin films. Physical Review B, 2000, 62, 1338-1349.	3.2	89
25	Contrast enhancement of rare-earth switchable mirrors through microscopic shutter effect. Applied Physics Letters, 1999, 75, 2050-2052.	3.3	86
26	Mg–Ti–H thin films for smart solar collectors. Applied Physics Letters, 2006, 88, 241910.	3.3	86
27	Nanostructured Pd–Au based fiber optic sensors for probing hydrogen concentrations in gas mixtures. International Journal of Hydrogen Energy, 2013, 38, 4201-4212.	7.1	80
28	Structural and optical properties ofMg2NiHxswitchable mirrors upon hydrogen loading. Physical Review B, 2004, 70, .	3.2	79
29	Suppressing H ₂ Evolution and Promoting Selective CO ₂ Electroreduction to CO at Low Overpotentials by Alloying Au with Pd. ACS Catalysis, 2019, 9, 3527-3536.	11.2	79
30	Seeing Hydrogen in Colors: Lowâ€Cost and Highly Sensitive Eye Readable Hydrogen Detectors. Advanced Functional Materials, 2014, 24, 2374-2382.	14.9	78
31	Flux creep and critical currents in epitaxial high Tc films. Cryogenics, 1990, 30, 563-568.	1.7	77
32	In-situ TEM on (de)hydrogenation of Pd at 0.5–4.5 bar hydrogen pressure and 20–400°C. Ultramicroscopy, 2012, 112, 47-52.	1.9	77
33	Solar Water Splitting Combining a BiVO ₄ Light Absorber with a Ru-Based Molecular Cocatalyst. Journal of Physical Chemistry C, 2015, 119, 7275-7281.	3.1	75
34	Extracting large photovoltages from a-SiC photocathodes with an amorphous TiO ₂ front surface field layer for solar hydrogen evolution. Energy and Environmental Science, 2015, 8, 1585-1593.	30.8	74
35	An optical method to determine the thermodynamics of hydrogen absorption and desorption in metals. Applied Physics Letters, 2007, 91, 231916.	3.3	73
36	Laser ablation threshold of YBa2Cu3O6+x. Applied Physics Letters, 1994, 65, 1581-1583.	3.3	72

#	Article	IF	CITATIONS
37	Epitaxial switchable yttrium-hydride mirrors. Applied Physics Letters, 1999, 75, 1724-1726.	3.3	69
38	Self-Organized Layered Hydrogenation in BlackMg2NiHxSwitchable Mirrors. Physical Review Letters, 2004, 93, 197404.	7.8	69
39	Interface Energy Controlled Thermodynamics of Nanoscale Metal Hydrides. Advanced Energy Materials, 2011, 1, 754-758.	19.5	68
40	The growth spiral morphology on {100} KDP related to impurity effects and step kinetics. Journal of Crystal Growth, 1986, 76, 243-250.	1.5	65
41	Optimization of Mg-based fiber optic hydrogen detectors by alloying the catalyst. International Journal of Hydrogen Energy, 2008, 33, 1084-1089.	7.1	64
42	Optical fiber sensor for the continuous monitoring of hydrogen in oil. Sensors and Actuators B: Chemical, 2014, 190, 982-989.	7.8	62
43	Plasmonic enhancement of the optical absorption and catalytic efficiency of BiVO4 photoanodes decorated with Ag@SiO2 core–shell nanoparticles. Physical Chemistry Chemical Physics, 2014, 16, 15272-15277.	2.8	61
44	Kinetic Roughening of Penetrating Flux Fronts in High-TcThin Film Superconductors. Physical Review Letters, 1999, 83, 2054-2057.	7.8	60
45	Nucleation and growth mechanisms of nano magnesium hydride from the hydrogen sorption kinetics. Physical Chemistry Chemical Physics, 2013, 15, 11501.	2.8	59
46	Oxynitrogenography: Controlled Synthesis of Single-Phase Tantalum Oxynitride Photoabsorbers. Chemistry of Materials, 2015, 27, 7091-7099.	6.7	59
47	Quasifree Mg–H thin films. Applied Physics Letters, 2009, 95, .	3.3	57
48	Photoelectrochemical Properties of Cadmium Chalcogenide-Sensitized Textured Porous Zinc Oxide Plate Electrodes. ACS Applied Materials & Interfaces, 2013, 5, 1113-1121.	8.0	57
49	Combinatorial thin film methods for the search of new lightweight metal hydrides. Scripta Materialia, 2007, 56, 853-858.	5.2	56
50	Vortex pinning by natural defects in thin films of YBa2Cu3O7â^'δ. Superconductor Science and Technology, 2002, 15, 395-404.	3.5	55
51	Photochromism of rare-earth metal-oxy-hydrides. Applied Physics Letters, 2017, 111, .	3.3	55
52	Hydrogenography of PdHx thin films: Influence of H-induced stress relaxation processes. Acta Materialia, 2009, 57, 1209-1219.	7.9	54
53	Catalytic activity of noble metals promoting hydrogen uptake. Journal of Catalysis, 2006, 239, 263-271.	6.2	53
54	Thermodynamics, stress release and hysteresis behavior inÂhighly adhesive Pd–H films. International Journal of Hydrogen Energy, 2011, 36, 4056-4067.	7.1	53

#	Article	IF	CITATIONS
55	Polymerâ€Induced Surface Modifications of Pdâ€based Thin Films Leading to Improved Kinetics in Hydrogen Sensing and Energy Storage Applications. Angewandte Chemie - International Edition, 2014, 53, 12081-12085.	13.8	53
56	Incommensurate Morphology of Calaverite (AuTe2) Crystals. Physical Review Letters, 1985, 55, 2301-2304.	7.8	52
57	The mechanism of tapering on KDP-type crystals. Journal of Crystal Growth, 1986, 74, 118-128.	1.5	52
58	Nanoscale composition modulations in MgyTi1â^'yHx thin film alloys for hydrogen storage. International Journal of Hydrogen Energy, 2009, 34, 1450-1457.	7.1	52
59	Mg/Ti multilayers: Structural and hydrogen absorption properties. Physical Review B, 2010, 81, .	3.2	52
60	Effect of the substrate on the thermodynamic properties of PdHx films studied by hydrogenography. Scripta Materialia, 2009, 60, 348-351.	5.2	50
61	Metal–organic framework thin films for protective coating of Pd-based optical hydrogen sensors. Journal of Materials Chemistry C, 2013, 1, 8146.	5.5	48
62	Metal hydrides for smart window and sensor applications. MRS Bulletin, 2013, 38, 495-503.	3.5	48
63	Metal-hydrogen systems with an exceptionally large and tunable thermodynamic destabilization. Nature Communications, 2017, 8, 1846.	12.8	47
64	Preparation, patterning, and properties of thin YBa2Cu3O7â^`Îfilms. Applied Physics Letters, 1988, 52, 1904-1906.	3.3	46
65	Unexpected fourfold symmetry in the resistivity of patterned superconductors. Physical Review B, 2003, 67, .	3.2	46
66	Oxyhydride Nature of Rare-Earth-Based Photochromic Thin Films. Journal of Physical Chemistry Letters, 2019, 10, 1342-1348.	4.6	45
67	Direct Comparison of PdAu Alloy Thin Films and Nanoparticles upon Hydrogen Exposure. ACS Applied Materials & Interfaces, 2019, 11, 15489-15497.	8.0	45
68	Growth and etching phenomena observed by STM/AFM on pulsed-laser deposited YBa2Cu3O7â^îŕ films. Physica C: Superconductivity and Its Applications, 1996, 261, 1-11.	1.2	44
69	Thin film metal hydrides for hydrogen storage applications. Journal of Materials Chemistry, 2011, 21, 4021-4026.	6.7	44
70	Post-synthetic cation exchange in the robust metal–organic framework MIL-101(Cr). CrystEngComm, 2013, 15, 10175.	2.6	44
71	Hysteresis and the role of nucleation and growth in the hydrogenation of Mg nanolayers. Physical Chemistry Chemical Physics, 2013, 15, 2782.	2.8	44
72	On the formation of etch grooves around stress fields due to inhomogeneous impurity distribution in KH2PO4 single crystals. Journal of Crystal Growth, 1981, 51, 607-623.	1.5	42

#	Article	IF	CITATIONS
73	Mechanism of incongruent ablation of SrTiO3. Journal of Applied Physics, 1998, 83, 3386-3389.	2.5	42
74	Mg–Ni–H films as selective coatings: Tunable reflectance by layered hydrogenation. Applied Physics Letters, 2004, 84, 3651-3653.	3.3	42
75	In situ electrochemical XRD study of (de)hydrogenation of MgyTi100â^'y thin films. Journal of Materials Chemistry, 2008, 18, 3680.	6.7	42
76	Strong pinning linear defects formed at the coherent growth transition of pulsed-laser-depositedYBa2Cu3O7â^îfilms. Physical Review B, 2002, 65, .	3.2	41
77	The role of niobium oxide as a surface catalyst for hydrogen absorption. Journal of Catalysis, 2005, 235, 353-358.	6.2	41
78	Mg–Ti–H thin films as switchable solar absorbers. International Journal of Hydrogen Energy, 2008, 33, 3188-3192.	7.1	41
79	Hafnium—an optical hydrogen sensor spanning six orders in pressure. Nature Communications, 2017, 8, 15718.	12.8	41
80	In situ observation of surface phenomena on {100} and {101} potassium dihydrogen phosphate crystals. Journal of Crystal Growth, 1984, 69, 306-316.	1.5	40
81	Study of the hydride forming process of in-situ grown MgH2 thin films by activated reactive evaporation. Thin Solid Films, 2008, 516, 4351-4359.	1.8	40
82	MOF@MOF core–shell vs. Janus particles and the effect of strain: potential for guest sorption, separation and sequestration. CrystEngComm, 2013, 15, 6003.	2.6	40
83	Optimization of amorphous silicon double junction solar cells for an efficient photoelectrochemical water splitting device based on a bismuth vanadate photoanode. Physical Chemistry Chemical Physics, 2014, 16, 4220-4229.	2.8	40
84	Effect of the strong metal-support interaction on hydrogen sorption kinetics of Pd-capped switchable mirrors. Physical Review B, 2004, 70, .	3.2	39
85	Hydrogen absorption kinetics and optical properties of Pd-doped Mg thin films. Journal of Applied Physics, 2006, 100, 023515.	2.5	39
86	Highly destabilized Mg-Ti-Ni-H system investigated by density functional theory and hydrogenography. Physical Review B, 2008, 77, .	3.2	39
87	Critical currents and magnetic relaxation of epitaxial YBa2Cu3O7 â^ î´ films. Journal of the Less Common Metals, 1989, 151, 39-48. Chemical short-range order and lattice deformations in <mml:math< td=""><td>0.8</td><td>37</td></mml:math<>	0.8	37
88	xmlns:mml="http://www.w3.org/1998/Math/MathML" display="inline"> <mml:mrow><mml:msub><mml:mi mathvariant="normal">Mg<mml:mi>y</mml:mi></mml:mi </mml:msub><mml:msub><mml:mi mathvariant="normal">Ti<mml:mrow><mml:mn>1</mml:mn><mml:mo>â^^</mml:mo><ml:mi>ymathvariant="normal">H<mml:mi>x</mml:mi></ml:mi></mml:mrow></mml:mi </mml:msub></mml:mrow> s	ımî:mi> <td>nml:mrow><!--</td--></td>	nml:mrow> </td
89	films probed by hydrogenography. Physical Review B, 2008, 77, . A novel approach for the preparation of textured CuO thin films from electrodeposited CuCl and CuBr. Journal of Electroanalytical Chemistry, 2014, 717-718, 243-249.	3.8	37
90	The morphology of calaverite (AuTe2) from data of 1931. Solution of an old problem of rational indices. Acta Crystallographica Section A: Foundations and Advances, 1989, 45, 115-123.	0.3	36

#	Article	IF	CITATIONS
91	Ti-catalyzed Mg(AlH4)2: A reversible hydrogen storage material. Journal of Alloys and Compounds, 2005, 404-406, 775-778.	5.5	36
92	Effect of the Deposition Technique on the Metallurgy and Hydrogen Storage Characteristics of Metastable Mg[sub y]Ti[sub (1â^'y)] Thin Films. Electrochemical and Solid-State Letters, 2006, 9, A520.	2.2	35
93	Gradient dopant profiling and spectral utilization of monolithic thin-film silicon photoelectrochemical tandem devices for solar water splitting. Journal of Materials Chemistry A, 2015, 3, 4155-4162.	10.3	35
94	Photoelectrochemical water splitting with porous α-Fe2O3 thin films prepared from Fe/Fe-oxide nanoparticles. Applied Catalysis A: General, 2016, 523, 130-138.	4.3	35
95	Structural and optical properties of MgxAl1-xHy gradient thin films: a combinatorial approach. Applied Physics A: Materials Science and Processing, 2006, 84, 77-85.	2.3	34
96	Influence of the Chemical Potential on the Hydrogen Sorption Kinetics of Mg2Ni/TM/Pd (TM =) Tj ETQq0 0 0 rgBT	/Qverlock	10 Tf 50 54
97	Opto-mechanical characterization of hydrogen storage properties of Mg–Ni thin film composition spreads. Applied Surface Science, 2007, 254, 682-686.	6.1	34
98	Thermal stability of gas phase magnesium nanoparticles. Journal of Applied Physics, 2010, 107, 053504.	2.5	34
99	Solid-State NMR Studies of the Photochromic Effects of Thin Films of Oxygen-Containing Yttrium Hydride. Journal of Physical Chemistry C, 2014, 118, 22935-22942.	3.1	34
100	Effect of the two (100) SrTiO3 substrate terminations on the nucleation and growth of YBa2Cu3O7â~'δ thin films. Physica C: Superconductivity and Its Applications, 2001, 351, 183-199.	1.2	33
101	Probing hydrogen spillover in Pd@MIL-101(Cr) with a focus on hydrogen chemisorption. Physical Chemistry Chemical Physics, 2014, 16, 5803.	2.8	33
102	Hydride destabilization in core–shell nanoparticles. International Journal of Hydrogen Energy, 2014, 39, 2115-2123.	7.1	33
103	Stabilized switchable "black state―in Mg2NiH4â^•Tiâ^•Pd thin films for optical hydrogen sensing. Applied Physics Letters, 2006, 89, 021913.	3.3	32
104	An optical hydrogen sensor based on a Pd-capped Mg thin film wedge. International Journal of Hydrogen Energy, 2010, 35, 12574-12578.	7.1	32
105	Combinatorial method for the development of a catalyst promoting hydrogen uptake. Journal of Alloys and Compounds, 2005, 404-406, 699-705.	5.5	31
106	Critical current density and pinning energy of an epitaxial YBa2Cu3O7-δfilm. Physica C: Superconductivity and Its Applications, 1989, 159, 854-862.	1.2	30
107	Positron depth profiling of the structural and electronic structure transformations of hydrogenated Mg-based thin films. Journal of Applied Physics, 2009, 105, .	2.5	30

108Destabilization of Mg Hydride by Self-Organized Nanoclusters in the Immiscible Mgâ€"Ti System. Journal
of Physical Chemistry C, 2015, 119, 12157-12164.3.130

#	Article	IF	CITATIONS
109	High-throughput concept for tailoring switchable mirrors. Applied Surface Science, 2006, 253, 1417-1423.	6.1	29
110	Optical, structural, and electrical properties of Mg2NiH4 thin films in situ grown by activated reactive evaporation. Journal of Applied Physics, 2006, 100, 063518.	2.5	29
111	Hydrogenography of Mg Ni1â^'H gradient thin films: Interplay between the thermodynamics and kinetics of hydrogenation. Acta Materialia, 2010, 58, 658-668.	7.9	29
112	Crossover between fractal and nonfractal flux penetration in high-temperature superconducting thin films. Physical Review B, 1998, 58, 12467-12477.	3.2	28
113	Titanium nitride: A new Ohmic contact material for n-type CdS. Journal of Applied Physics, 2011, 110, .	2.5	28
114	Metal Hydride Based Optical Hydrogen Sensors. Journal of the Physical Society of Japan, 2020, 89, 051003.	1.6	28
115	Tantalumâ€Palladium: Hysteresisâ€Free Optical Hydrogen Sensor Over 7 Orders of Magnitude in Pressure with Subâ€Second Response. Advanced Functional Materials, 2021, 31, 2010483.	14.9	28
116	A superspace approach to the structure and morphology of tetramethylammonium tetrachlorozincate, 2C4H12N+.ZnCl4 2â^'. Acta Crystallographica Section B: Structural Science, 1986, 42, 69-77.	1.8	27
117	Resistive states in thin films of Y2Ba4Cu8O16â~δ. Physica C: Superconductivity and Its Applications, 1990, 167, 348-358.	1.2	27
118	The transition from 2D-nucleation to spiral growth in pulsed laser deposited YBa2Cu3O7â^î´ films. Physica C: Superconductivity and Its Applications, 1998, 305, 1-10.	1.2	27
119	A simple route for preparation of textured WO3 thin films from colloidal W nanoparticles and their photoelectrochemical water splitting properties. Applied Catalysis B: Environmental, 2015, 166-167, 406-412.	20.2	27
120	Optical hydrogen sensing with nanoparticulate Pd–Au films produced by spark ablation. Sensors and Actuators B: Chemical, 2015, 221, 290-296.	7.8	26
121	Optical hydrogen sensing beyond palladium: Hafnium and tantalum as effective sensing materials. Sensors and Actuators B: Chemical, 2019, 283, 538-548.	7.8	26
122	Growth mode issues in epitaxy of complex oxide thin films. Journal of Materials Science: Materials in Electronics, 1998, 9, 217-226.	2.2	25
123	Hydrogen sorption mechanism of oxidized nickel clusters. Applied Physics Letters, 2004, 85, 4884-4886.	3.3	25
124	Electrohydrogenation of MgH2-thin films. Applied Physics Letters, 2007, 90, 071912.	3.3	25
125	Stoichiometric transfer of complex oxides by pulsed laser deposition. Applied Surface Science, 1996, 96-98, 679-684.	6.1	24
126	Structural and optical properties of MgyNi1–yHx gradient thin films in relation to the as-deposited metallic state. International Journal of Hydrogen Energy, 2009, 34, 8951-8957.	7.1	24

BERNARD DAM

#	Article	IF	CITATIONS
127	Functionalised metal–organic frameworks: a novel approach to stabilising single metal atoms. Journal of Materials Chemistry A, 2017, 5, 15559-15566.	10.3	24
128	Thin film based sensors for a continuous monitoring of hydrogen concentrations. Sensors and Actuators B: Chemical, 2012, 165, 88-96.	7.8	23
129	Impact of Nanostructuring on the Phase Behavior of Insertion Materials: The Hydrogenation Kinetics of a Magnesium Thin Film. Journal of Physical Chemistry C, 2016, 120, 10185-10191.	3.1	23
130	Elastic versus Alloying Effects in Mg-Based Hydride Films. Physical Review Letters, 2018, 121, 255503.	7.8	23
131	Interplay of Linker Functionalization and Hydrogen Adsorption in the Metal–Organic Framework MIL-101. Journal of Physical Chemistry C, 2014, 118, 19572-19579.	3.1	22
132	Flux-creep and critical currents in various YBaCuO-samples. Physica C: Superconductivity and Its Applications, 1988, 153-155, 322-323.	1.2	21
133	Triode-Sputtered High- <i>T</i> _c Superconducting Thin Films. Europhysics Letters, 1988, 5, 455-460.	2.0	21
134	NonlinearU(j) dependence determined directly from low-electric-fieldE-jscurves inYBa2Cu3O7â^'δthin films. Physical Review B, 1995, 52, 4583-4587.	3.2	21
135	The growth-induced microstructural origin of the optical black state of Mg2NiHx thin films. Journal of Alloys and Compounds, 2006, 416, 2-10.	5.5	21
136	Divacancies and the hydrogenation of Mg-Ti films with short range chemical order. Applied Physics Letters, 2010, 96, .	3.3	21
137	X-ray photoelectron spectroscopy investigation of magnetron sputtered Mg–Ti–H thin films. International Journal of Hydrogen Energy, 2013, 38, 10704-10715.	7.1	21
138	Fiber optic hydrogen sensor for a continuously monitoring of the partial hydrogen pressure in the natural gas grid. Sensors and Actuators B: Chemical, 2014, 199, 127-132.	7.8	21
139	A "rough heart―model for "edge―dislocations which act as persistent growth sources. Journal of Crystal Growth, 1984, 67, 400-403.	1.5	20
140	In SituObservation of a Roughening Transition of the (1012Â ⁻) Satellite Crystal Surface of Modulated ((CH3)N4)Zn2Cl4. Physical Review Letters, 1985, 55, 2806-2809.	7.8	20
141	High critical currents and flux creep effects in superconducting YBa2Cu3O7 â~' gd films e-gun deposited using a BaF2 source. Journal of the Less Common Metals, 1989, 151, 325-331.	0.8	20
142	Mechanism of the structural phase transformations in epitaxial YHx switchable mirrors. Journal of Applied Physics, 2002, 91, 1901-1909.	2.5	20
143	The dielectric function of Mgy NiHx thin films (). Journal of Alloys and Compounds, 2007, 430, 13-18.	5.5	20
	Optical response of the sodium alanate system: <mml:math< td=""><td></td><td></td></mml:math<>		

144

xmlns:mml="http://www.w3.org/1998/Math/Math/ML" display="inline"><mml:mrow><mml:msub><mml:mi mathvariant="italic">GW</mml:mi><mml:mrow><mml:mn>0</mml:mn></mml:mrow></mml:msub></mml:msub></mml:mrow></mml:math>-BSE calculations and thin film measurements. Physical Review B, 2011, 83, .

#	Article	IF	CITATIONS
145	Thermodynamic Properties, Hysteresis Behavior and Stress-Strain Analysis of MgH2 Thin Films, Studied over a Wide Temperature Range. Crystals, 2012, 2, 710-729.	2.2	20
146	Structure Model for Anion-Disordered Photochromic Gadolinium Oxyhydride Thin Films. Journal of Physical Chemistry C, 2020, 124, 13541-13549.	3.1	20
147	The transition from 2D-nucleation to spiral growth in pulsed laser deposited YBa2Cu3O7â^Î^ films. Physica C: Superconductivity and Its Applications, 1998, 296, 179-187.	1.2	19
148	Promotion of Hydrogen Desorption from Palladium Surfaces by Fluoropolymer Coating. ChemCatChem, 2016, 8, 1646-1650.	3.7	19
149	Influence of Cation (RE = Sc, Y, Gd) and O/H Anion Ratio on the Photochromic Properties of REO _{<i>x</i>} H _{3–2<i>x</i>} Thin Films. ACS Photonics, 2021, 8, 709-715.	6.6	19
150	Observation of Bands of Faces on IncommensurateRb2ZnBr4Single Crystals. Physical Review Letters, 1983, 50, 849-852.	7.8	18
151	Magnetic flux relaxation of epitaxial YBa 2 Cu 3 O 7-δ films at low temperatures Physica C: Superconductivity and Its Applications, 1989, 162-164, 663-664.	1.2	18
152	Magneto-optical investigation of flux penetration in a superconducting ring. Physical Review B, 2001, 64, .	3.2	18
153	Double layer formation in Mg–TM switchable mirrors (TM: Ni, Co, Fe). Journal of Alloys and Compounds, 2005, 404-406, 490-493.	5.5	18
154	Photocorrosion Mechanism of TiO ₂ -Coated Photoanodes. International Journal of Photoenergy, 2015, 2015, 1-8.	2.5	18
155	The laser ablation threshold of YBa2Cu3O6+x as revealed by using projection optics. Applied Surface Science, 1995, 86, 13-17.	6.1	17
156	High-quality off-stoichiometric YBa2Cu3O7â^'δ films produced by diffusion-assisted preferential laser ablation. Journal of Applied Physics, 1999, 86, 6528-6537.	2.5	17
157	Temperature and magnetic-field dependence of quantum creep in various high-Tcsuperconductors. Physical Review B, 1999, 59, 7222-7237.	3.2	17
158	High throughput screening of Pd-alloys for H2 separation membranes studied by hydrogenography and CVM. International Journal of Hydrogen Energy, 2011, 36, 1074-1082.	7.1	17
159	Wavelength response of a surface plasmon resonance palladium-coated optical fiber sensor for hydrogen detection. Optical Engineering, 2011, 50, 014403.	1.0	17
160	Highly sensitive and selective visual hydrogen detectors based on YxMg1â^'x thin films. Sensors and Actuators B: Chemical, 2014, 203, 745-751.	7.8	17
161	The effect of microstructure on the hydrogenation of Mg/Fe thin film multilayers. International Journal of Hydrogen Energy, 2014, 39, 17092-17103.	7.1	17
162	Amorphous Metal-Hydrides for Optical Hydrogen Sensing: The Effect of Adding Glassy Ni–Zr to Mg–Ni–H. ACS Sensors, 2016, 1, 222-226.	7.8	17

#	Article	IF	CITATIONS
163	Morphological determination of modulated-cell parameters of Rb ₂ ZnBr ₄ . Zeitschrift Für Kristallographie, 1983, 165, 247-254.	1.1	16
164	Transmission electron microscopy of thin YBa2Cu3O7â^'x films on (001) SrTiO3 prepared by DC triode sputtering. Journal of Crystal Growth, 1988, 91, 355-362.	1.5	16
165	Magnetic and transport properties of sputtered La0.67Ca0.33MnO3 thin films. Journal of Magnetism and Magnetic Materials, 1997, 165, 380-382.	2.3	16
166	The hydrogen permeability of Pd–Cu based thin film membranes in relation to their structure: A combinatorial approach. International Journal of Hydrogen Energy, 2015, 40, 3932-3943.	7.1	16
167	The Impact of Post-Synthetic Linker Functionalization of MOFs on Methane Storage: The Role of Defects. Frontiers in Energy Research, 2016, 4, .	2.3	16
168	Buffer layers for superconducting Yî—,Baî—,Cuî—,O thin films on silicon and SiO2. Materials Science and Engineering B: Solid-State Materials for Advanced Technology, 1990, 7, 135-147.	3.5	15
169	Siting and Mobility of Deuterium Absorbed in Cosputtered Mg0.65Ti0.35. A MAS 2H NMR Study. Journal of Physical Chemistry C, 2011, 115, 288-297.	3.1	15
170	A synchrotron radiation study of modulated [(CH3)4N]2ZnCl4 crystals. Journal of Applied Crystallography, 1987, 20, 512-516.	4.5	14
171	RBS-PIXE analysis on μm scale on thin film high-Tc superconductors. Nuclear Instruments & Methods in Physics Research B, 1994, 89, 204-207.	1.4	14
172	The relation between the defect structure, the surface roughness and the growth conditions of YBa2Cu3O7â^1´films. Journal of Alloys and Compounds, 1997, 251, 27-30.	5.5	14
173	Local switching in epitaxialYHxswitchable mirrors. Physical Review B, 2002, 65, .	3.2	13
174	Electrical and optical properties of epitaxial YHx switchable mirrors. Journal of Alloys and Compounds, 2005, 397, 9-16.	5.5	13
175	Lightweight sodium alanate thin films grown by reactive sputtering. Applied Physics Letters, 2009, 95, 121904.	3.3	13
176	EXAFS investigation of the destabilization of the Mg–Ni–Ti (H) system. International Journal of Hydrogen Energy, 2012, 37, 4161-4169.	7.1	13
177	Electronic structure and vacancy formation in photochromic yttrium oxy-hydride thin films studied by positron annihilation. Solar Energy Materials and Solar Cells, 2018, 177, 97-105.	6.2	13
178	Polymer Modification of Surface Electronic Properties of Electrocatalysts. ACS Energy Letters, 2022, 7, 1586-1593.	17.4	13
179	Morphology of modulated crystals and quasicrystals. Journal Physics D: Applied Physics, 1991, 24, 186-198.	2.8	12
180	Angular scaling of critical current measurements on laser-ablated YBa2Cu3O7â^î^ thin films. Physica C: Superconductivity and Its Applications, 1994, 235-240, 3053-3054.	1.2	12

#	Article	IF	CITATIONS
181	Magnetic force microscopy of vortex pinning at grain boundaries in superconducting thin films. Physica C: Superconductivity and Its Applications, 2002, 369, 165-170.	1.2	12
182	In situ preparation of YH2 thin films by PLD for switchable devices. Journal of Alloys and Compounds, 2003, 356-357, 526-529.	5.5	12
183	Layer-resolved study of the Mg to MgH2 transformation in Mg–Ti films with short-range chemical order. Journal of Alloys and Compounds, 2011, 509, S567-S571.	5.5	12
184	Interface and strain effects on the H-sorption thermodynamics of size-selected Mg nanodots. International Journal of Hydrogen Energy, 2016, 41, 9841-9851.	7.1	12
185	Effect of the addition of zirconium on the photochromic properties of yttrium oxy-hydride. Solar Energy Materials and Solar Cells, 2019, 200, 109923.	6.2	12
186	Thermally activated flux motion in high-T c superconductors. Physica C: Superconductivity and Its Applications, 1989, 162-164, 1191-1192.	1.2	11
187	Thermally activated flux motion and quantum creep in YBa2Cu3O7 and Y2Ba4Cu8O16 films. Journal of Alloys and Compounds, 1993, 195, 427-430.	5.5	11
188	In-Situ Deposition of Alkali and Alkaline Earth Hydride Thin Films To Investigate the Formation of Reactive Hydride Composites. Journal of Physical Chemistry C, 2010, 114, 13895-13901.	3.1	11
189	Enhancement of Destabilization and Reactivity of Mg Hydride Embedded in Immiscible Ti Matrix by Addition of Cr: Pd-Free Destabilized Mg Hydride. Journal of Physical Chemistry C, 2017, 121, 12631-12635.	3.1	11
190	Growth and hydrogenation of epitaxial yttrium switchable mirrors on CaF2. Thin Solid Films, 2002, 402, 131-142.	1.8	10
191	Optical hydrogen sensors based on metal-hydrides. Proceedings of SPIE, 2012, , .	0.8	10
192	Crystal form and surface morphology of modulated β-K2SO4-type structures. Acta Crystallographica Section B: Structural Science, 1987, 43, 64-71.	1.8	9
193	Twin-free YBa2Cu3O7â~δ films on (001) NdGaO3 showing isotropic electrical behaviour. Journal of Alloys and Compounds, 1997, 251, 114-117.	5.5	9
194	Effect of H-induced microstructural changes on pressure-optical transmission isotherms for Mg–V thin films. International Journal of Hydrogen Energy, 2010, 35, 6959-6970.	7.1	9
195	Ni and p-Cu2O Nanocubes with a Small Size Distribution by Templated Electrodeposition and Their Characterization by Photocurrent Measurement. ACS Applied Materials & Interfaces, 2013, 5, 10938-10945.	8.0	9
196	Single Quality Factor for Enthalpyâ€Entropy Compensation, Isoequilibrium and Isokinetic Relationships. ChemPhysChem, 2020, 21, 1632-1643.	2.1	9
197	Structural properties and anion dynamics of yttrium dihydride and photochromic oxyhydride thin films examined by <i>in situ</i> <mml:math xmlns:mml="http://www.w3.org/1998/Math/MathML"><mml:mrow><mml:msup><mml:mi>μ</mml:mi><mml:rephysical .<="" 103,="" 2021,="" b,="" review="" td=""><td>no3:2<td>nl:mo></td></td></mml:rephysical></mml:msup></mml:mrow></mml:math>	no3: 2 <td>nl:mo></td>	nl:mo>
198	Simple Accurate Verification of Enthalpyâ€Entropy Compensation and Isoequilibrium Relationship. ChemPhysChem, 2021, 22, 1774-1784.	2.1	9

#	Article	IF	CITATIONS
199	Influence of micro-structure in the low temperature critical currents of YBa2Cu3O7?? thin films. Journal of Low Temperature Physics, 1996, 105, 1017-1022.	1.4	8
200	Critical composition dependence of the hydrogenation of Mg2±δ Ni thin films. Journal of Alloys and Compounds, 2007, 428, 34-39.	5.5	8
201	Thermal Stability of MgyTi1-y Thin Films Investigated by Positron Annihilation Spectroscopy. Physics Procedia, 2012, 35, 16-21.	1.2	8
202	The clamping effect in the complex hydride Mg2NiH4 thin films. Journal of Materials Chemistry A, 2013, 1, 10972.	10.3	8
203	Influence of Crystal Structure, Encapsulation, and Annealing on Photochromism in Nd Oxyhydride Thin Films. Journal of Physical Chemistry C, 2022, 126, 2276-2284.	3.1	8
204	Relation between micro-structure and transport properties of epitaxial YBa2Cu3O7â^Î^thin films. Physica C: Superconductivity and Its Applications, 1997, 282-287, 2303-2304.	1.2	7
205	Microstructural origin of the optical black state in Mg2NiHx thin films. Journal of Alloys and Compounds, 2005, 404-406, 481-484.	5.5	7
206	Magnesium Nanoparticles for Hydrogen Storage: Structure, Kinetics and Thermodynamics. IOP Conference Series: Materials Science and Engineering, 2012, 38, 012001.	0.6	7
207	Hydrogen diffusion through Ru thin films. International Journal of Hydrogen Energy, 2020, 45, 15003-15010.	7.1	7
208	Controlling the natural strong pinning sites in laser ablated YBa2Cu3O7-δ thin films. Physica C: Superconductivity and Its Applications, 2000, 341-348, 2327-2330.	1.2	6
209	Thermochromic metal-hydride bilayer devices. Journal of Alloys and Compounds, 2005, 404-406, 465-468.	5.5	6
210	Combined XPS and first principle study of metastable Mg–Ti thin films. Surface and Interface Analysis, 2012, 44, 986-988.	1.8	6
211	Suppression of the Phase Coexistence of the fcc–fct Transition in Hafnium-Hydride Thin Films. Journal of Physical Chemistry Letters, 2021, 12, 10969-10974.	4.6	6
212	Formation of vacancies and metallic-like domains in photochromic rare-earth oxyhydride thin films studied by <i>in-situ</i> illumination positron annihilation spectroscopy. Physical Review Materials, 2022, 6, .	2.4	6
213	The ab-anisotrophy of twinfree YBa2Cu3O7-δ films above and below Tc. Physica C: Superconductivity and Its Applications, 1997, 282-287, 665-666.	1.2	5
214	Growth-Induced Strong Pinning Sites in Laser Ablated YBa2Cu3O7-δ Films with a Non-Random Distribution. Journal of Low Temperature Physics, 1999, 117, 663-667.	1.4	5
215	In situ monitoring of optical and structural switching in epitaxial YHx switchable mirrors. Journal of Alloys and Compounds, 2002, 330-332, 342-347.	5.5	5
216	The properties of pulsed laser deposited YH2 films for switchable devices. Journal of Alloys and Compounds, 2003, 356-357, 536-540.	5.5	5

#	Article	IF	CITATIONS
217	Infinite-layer copper-oxide laser-ablated thin films: substrate, buffer-layer, and processing effects. IEEE Transactions on Applied Superconductivity, 2003, 13, 2684-2686.	1.7	5
218	Combinatorial method for direct measurements of the intrinsic hydrogen permeability of separation membrane materials. Journal of Membrane Science, 2013, 444, 70-76.	8.2	5
219	Unveiling Nanoscale Compositional and Structural Heterogeneities of Highly Textured Mg0.7Ti0.3Hy Thin Films. Inorganic Chemistry, 2020, 59, 6800-6807.	4.0	5
220	Nanostructural Perspective for Destabilization of Mg Hydride Using the Immiscible Transition Metal Mn. Inorganic Chemistry, 2021, 60, 15024-15030.	4.0	5
221	Photochromic YO _x H _y Thin Films Examined by <i>in situ</i> Positron Annihilation Spectroscopy. Acta Physica Polonica A, 2020, 137, 205-208. Energy, metastability, and optical properties of anion-disordered <mml:math< td=""><td>0.5</td><td>5</td></mml:math<>	0.5	5
222	xmlns:mml="http://www.w3.org/1998/Math/MathML"> <mml:mrow> <mml:mi>R</mml:mi> <mml:msub> <mml:mi mathvariant="normal">O <mml:mi>x</mml:mi> </mml:mi </mml:msub> <mml:msub> <mml:mi mathvariant="normal">H <mml:mrow> <mml:mn>3</mml:mn> <mml:mo> â^`</mml:mo> <mml:mn>2<mml:math< td=""><td>ıml:mn><</td><td>mml:mi>x</td></mml:math<></mml:mn></mml:mrow></mml:mi </mml:msub></mml:mrow>	ıml:mn><	mml:mi>x

#	Article	IF	CITATIONS
235	Influence of film growth conditions on the transport properties of YBa2Cu3O7â~δ step-edge junctions. Applied Superconductivity, 1997, 5, 249-254.	0.5	2
236	Pattern formation due to non-linear vortex diffusion. Physica C: Superconductivity and Its Applications, 2000, 341-348, 1011-1014.	1.2	2
237	Observation of step-flow growth in laser-ablated thin films of the T′-phase compound Pr2CuO4. Physica C: Superconductivity and Its Applications, 2000, 341-348, 2355-2356.	1.2	2
238	The noise characteristics of YBCO films with strong pinning. Technical Physics Letters, 2000, 26, 1078-1080.	0.7	2
239	Xâ€ray photoelectron spectroscopy study of MgH ₂ thin films grown by reactive sputtering. Surface and Interface Analysis, 2010, 42, 1140-1143.	1.8	2
240	Deposition of conductive TiN shells on SiO2 nanoparticles with a fluidized bed ALD reactor. Journal of Nanoparticle Research, 2016, 18, 1.	1.9	2
241	Designing Reliable Operando TEM Experiments to Study (De)lithiation Mechanism of Battery Electrodes. Journal of the Electrochemical Society, 2019, 166, A3384-A3386.	2.9	2
242	Metallurgical Synthesis of Mg2FexSi1–x Hydride: Destabilization of Mg2FeH6 Nanostructured in Templated Mg2Si. Inorganic Chemistry, 2020, 59, 2758-2764.	4.0	2
243	NATURE OF SHARP TEMPERATURE DEPENDENCY OF NORMAL PHASE FLICKER NOISE OF EPITAXIAL YBA2CU3O7-X FILMS. , 2001, , .		2
244	Electron tunnelling and critical current behaviour of patterned Y1Ba2Cu3O7 â~' δfilms. Journal of the Less Common Metals, 1989, 151, 435-441.	0.8	1
245	Magneto-optical observation of the influence of an artificial periodic magnetic pattern on the pinning of a YBa2Cu3O7â~δ thin film. Physica C: Superconductivity and Its Applications, 2000, 341-348, 1019-1022.	1.2	1
246	Vortex Pinning Regimes in thin films of YBa2Cu3O7â^îî. Physica C: Superconductivity and Its Applications, 2000, 341-348, 1463-1464.	1.2	1
247	Temperature dependence of the surface morphology of sputtered YBa2Cu3O7films. Superconductor Science and Technology, 2002, 15, 296-301.	3.5	1
248	Optimization of Pd surface plasmon resonance sensors for hydrogen detection. , 2011, , .		1
249	Innovative fiber optic sensor for hydrogen detection. , 2012, , .		1
250	Study of a fiber optic sensor for hydrogen leak detection. , 2013, , .		1
251	Contaminant-resistant MOF–Pd composite for H ₂ separation. RSC Advances, 2015, 5, 89323-89326.	3.6	1
252	Hydrogen Sensors: Tantalumâ€Palladium: Hysteresisâ€Free Optical Hydrogen Sensor Over 7 Orders of Magnitude in Pressure with Subâ€Second Response (Adv. Funct. Mater. 16/2021). Advanced Functional Materials, 2021, 31, 2170110.	14.9	1

#	Article	IF	CITATIONS
253	CRITICAL CURRENTS AND MAGNETIC RELAXATION OF EPITAXIAL YBa2Cu3O7–δ FILMS. , 1989, , 39-48.		1
254	Strong Pinning Mechanisms in High-Tc Superconducting Yba2Cu3O7-δThin Films. , 1999, , 331-343.		1
255	Low temperature fluxline relaxation effects in YBa2Cu3O7â^îî´thin films. Vacuum, 1990, 41, 862-863.	3.5	0
256	Critical currents and micro-structure in YBa2Cu3O7â^ʾî́ thin films. European Physical Journal D, 1996, 46, 1307-1308.	0.4	0
257	Title is missing!. Journal of Low Temperature Physics, 1999, 117, 1549-1553.	1.4	0
258	YBa2Cu3O7â^'δ films with self-organized natural linear defects. Physica C: Superconductivity and Its Applications, 2000, 341-348, 1985-1986.	1.2	0
259	A distributed optical fiber sensor for hydrogen detection based on Pd, and Mg alloys. Proceedings of SPIE, 2010, , .	0.8	0
260	ELECTRON TUNNELLING AND CRITICAL CURRENT BEHAVIOUR OF PATTERNED Y1Ba2Cu3O7–δFILMS. , 1989, , 435-441.		0
261	Stoichiometric transfer of complex oxides by pulsed laser deposition. , 1996, , 679-684.		0
262	Anisotropy Induced Crossover from Fractal to Non-Fractal Flux Penetration in High-Tc thin Films. , 1999, , 291-306.		0
263	Searching for Ti-clusters in Mg0.7Ti0.3 thin film. Acta Crystallographica Section A: Foundations and Advances, 2016, 72, s159-s159.	0.1	0